

# Analysis of long distance wakes behind a row of turbines - a parameter study

**O Eriksson, K Nilsson, S-P Breton, S Ivanell**

Wind Energy Campus Gotland, Dep. of Earth Sciences, Uppsala University, 621 67, Visby, Sweden

E-mail: [ola.eriksson@geo.uu.se](mailto:ola.eriksson@geo.uu.se)

## **Abstract.**

Large Eddy Simulations (LES) of the long distance wake behind a row of 10 turbines are conducted to predict wake recovery. The Navier-Stokes solver EllipSys3D is used in combination with the actuator disc concept. Neutral atmospheric conditions are assumed in combination with synthetic turbulence using the Mann method. Both the wind shear profile and turbulence are introduced into the flow field using body forces.

Previous simulations using the same simulation method to model the Horns Rev wind farm showed a higher wake recovery at long distances compared to measurements. The current study investigates further the sensitivity to parameters such as the grid resolution, Reynolds number, the turbulence characteristics as well as the impact of using different internal turbine spacings.

The clearest impact on the recovery behind the farm could be seen from the turbulence intensity of the incoming flow. The impact of the wind shear on the turbulence intensity in the domain needs further studies. A lower turbulence level gives slower wake recovery as expected. A slower wake recovery can also be seen for a higher grid resolution. The Reynolds number, apart from when using a very low value, has a small impact on the result. The variation of the internal spacing is seen to have a relatively minor impact on the farm wake recovery.

## **1. Introduction**

Large offshore wind farms are known to produce long distance wakes [1]. As many offshore wind farms are built, there will be more occasions when the wake from one wind farm will interact with other neighbouring wind farms. As a first step towards a better understanding of farm to farm interaction, numerical simulations are performed to study how well the modeling predicts the wake recovery behind single wind farms.

For wakes behind wind turbines and interaction inside wind farms one can find a wide range of studies. For an extensive list of different wake models, the reader is referred to Crespo et al. [2] and Vermeer et al. [3]. For a comparison of wake models with measurement data, here the Horns Rev wind farm, we refer to Barthelmie et al. [4].

Work in the field of wake modeling using Large Eddy Simulations (LES) has been performed, among others, by Ivanell et al. [5], Lu and Porté-Agel [6], Wu and Porté-Agel [7], Troldborg et al. [8][9], Keck et al. [10], Troldborg et al. [11] and Nilsson et al. [12].

Inside the farm CFD calculations employing the actuator disc methodology (ACD) combined with LES have been used to model the wakes. The simulations of the Horns Rev wind farm, by Ivanell [5], showed fairly good correlation concerning the power production inside the farm. Nilsson et al. [12] performed ACD simulations on the Lillgrund wind farm, showing that the relative power predicted by the simulations agreed very well with measurements.



Earlier studies of wake recovery at long distances behind whole wind farms have been done with different wake models and mesoscale simulations [1][13]. LES simulations using the ACD method extended to include the farm wake for Horns Rev wind farm were done by Eriksson [14]. The simulations showed a faster wake recovery at long distances compared to measurements.

The conditions for application of LES simulations using the ACD method for long distance wakes need to be further investigated. The current study investigates to what extent the results are impacted by parameters such as the grid resolution, Reynolds number, the turbulence characteristics as well as different internal turbine spacings. The relative power production, the long distance wake recovery and downstream development of turbulence are the main results to be studied.

The present study investigates the relative power production of a row of 10 turbines and the flow recovery downstream of the turbines when adjusting different simulation parameters (described in Section 4). While a similar study was recently conducted on a row of 10 turbines with focus on the conditions inside the farm [15], the present study focuses on the conditions behind the farm. The results are not directly comparable to real cases. The reasons for this is that the settings for the parametric study (described in Section 3) do not fully correspond to any real case, however some cases are close to the Horns Rev and Lillgrund wind farm for comparison. The aim is here to study the sensibility and trends in results with different parameter settings for simulations of long distance wakes.

## 2. Simulations of a row of 10 wind turbines

Simulations are performed for an incoming wind aligned with the row of 10 turbines, with rotor radius  $R$ , giving a full wake case, see Figure 1. The incoming wind speed ( $U$ ) at hub height is 8 m/s. The production of the turbines is studied and the wind is measured with probes at 0.5 internal spacing after each turbine. Additional probes measure the wind each km downstream in the farm wake up to 6 km behind the wind farm. The relative production and power coefficient are studied for the turbines. From the probe data, recorded every time step, the wind speed in the flow direction and the turbulence intensity are calculated.



**Figure 1.** The axial wind speed at hub height for a row of turbines with the internal spacing  $14 R$ . The upper part covers the first part of the domain and continues (behind the row) in the lower part showing the farm wake in which each km ( $21.5 R$ ) is marked with circles.

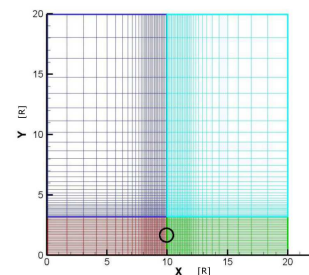


**Figure 2.** The equidistant region of the grid is  $4 R \times 4 R$ . The disc is shown by the circle.

## 3. Numerical model and simulation setup

Large Eddy Simulations (LES) are conducted using the Navier-Stokes solver EllipSys3D in combination with the actuator disc concept (ACD) [16]. The simulations are performed in non-dimensional form by normalizing with the rotor radius ( $R$ ) and incoming wind speed ( $U$ ). Neutral atmospheric conditions are assumed in combination with synthetic turbulence using the Mann method [17]. Both the wind shear profile and turbulence are introduced into the flow field using body forces [11]. The unresolvable turbulence scales are modeled through the eddy viscosity sub-grid-scale model, developed by Ta Phouc [18].

The settings of the simulations, e.g. choice of turbine, hub height, turbulence levels, wind shear, internal spacing, etc. are set to be close to or in between the values for the two existing wind farms Horns Rev and Lillgrund, see below for more detailed information. A detailed description of the setup and flow conditions at the Horns Rev wind farm is provided by Hansen et al. [19]. A description of the Lillgrund wind farm is given by Nilsson et al. [12].

### 3.1. Grid and boundary conditions

The grid is equidistant in  $4 R \times 4 R$ , see Figure 2. The inlet is stretched up to 15 R before the streamwise (z) equidistant region starts. In the lateral direction (x) the grid is stretched towards both sides and in the vertical direction (y) towards the top giving a grid covering  $20 R \times 20 R \times$  "length of domain". The length of the domain covers at least 6000 m behind the farm. The boundary condition in the inlet is fixed value, the top has far field, the sides cyclic conditions while the outlet has Dirichlet conditions and the ground boundary condition is no slip. The inlet values and the value on the top boundary follows the wind shear defined below.

### 3.2. Turbine and airfoil data

The turbines are implemented as body forces from tabulated airfoil data [16]. The airfoil data correspond to the Siemens SWT93-2.3 MW. The turbine is based on the NREL 5MW turbine [20] and downscaled to the wanted characteristics [12]. The turbine aims to run at the optimal tip speed ratio according to the used control strategy [21].

The chosen turbine with 2.3 MW rated power and a radius (R) of 46.5 m is the same as used in Lillgrund (compared to the Vestas V80, 2 MW, R 40 m used at Horns Rev). The used hub height is 1.6 R (compared to 1.46 R at Lillgrund and 1.76 R at Horns Rev).

### 3.3. Wind shear and turbulence

A wind shear is introduced into the domain as body forces in a prestep [11]. The used wind shear follows the power law with the shear exponent  $\alpha = 0.1$ . This can be compared to  $\alpha = 0.11$  used at Lillgrund [12] and  $\alpha = 0.15$  at Horns Rev (for inflow angle 270 degrees) [14]. For heights below 0.4 R a parabolic profile is used.

Turbulence is introduced as body forces from the Mann model [17][11]. The turbulence level is updated by adjusting the value of  $\alpha \epsilon^{2/3} [m^{4/3}s^{-2}]$  calculated from the roughness length and the wind speed 8 m/s at the hub height 74.4 m. The other parameters in the model are fixed with the eddy lifetime constant  $\gamma = 3.886$  and the length scale  $L = 43.9307 [m]$ . The spectra has been fitted to a Kaimal spectra. For a detailed description the reader is referred to Mann[22].

The turbulence intensity of the incoming flow (the background turbulence level) is measured in the empty CFD domain over 10 minutes at the rotor hub position of the first turbine. The turbulence intensity is defined as the standard deviation of the streamwise wind velocity normalized with the mean axial wind velocity. Turbulence is introduced at 17 R (from the inlet) and 4 R before the first turbine placed at 21 R. The turbulence is saved as a box that has  $16 \times 16 \times 512$  points covering  $4 \times 4 R$  with a vertical/lateral resolution of 0.25 R. Taylor frozen turbulence hypothesis is used to see the length of the turbulence box as a time series of turbulence planes introduced in the domain. The length of the box corresponds to a 10 minute time series for the wind speed 8 m/s. This gives a resolution of 9.375 m/0.2 R and a computational time step of 0.2016.

The turbulence intensity of 6.3 % is used as default. This can be compared to around 5 % for an inflow angle of 222 degrees at Lillgrund and 7 % for an angle of 270 degrees at Horns Rev.

### 3.4. Simulation times and time steps

The used simulation time allows the turbines to stabilize at the correct tip speed ratio and the turbulence to pass through the entire domain with the speed 8 m/s. After that it is averaged

over a number of steps corresponding to 20 minutes or two turbulence boxes. The time step is set to 0.25 of the CFL condition (for the incoming wind) in order to conservatively fulfill it.

#### 4. Parameter study

In order to find suitable settings for performing simulations of long distance wakes, the impact of different parameters needs to be studied. Here the grid resolution ( $dx$ ), Reynolds number ( $Re$ ), turbulence intensity ( $TI$ ) and internal spacing ( $dS$ ) are studied.

The values for the parameters are set to the same values used by Eriksson for the study of the wake behind Horns Rev [14] and varied one at the time. The standard values are:  $dx = 0.1$  R,  $Re = 50000$ ,  $TI = 6\%$  and  $dS = 14$  R.

##### 4.1. Grid resolution

The grid resolution impacts the numerical discretization error as well as the size of the smallest eddies that can be resolved instead of being handled by the sub grid scale model. For the Lillgrund study a resolution of 0.1 R was shown to be sufficient to study the relative production [12]. Here the impact of resolution with larger internal spacing and the impact on the long distance wake behind the farm will also be studied. The values will be varied in accordance to Table 1 with the reference resolution set to 0.1 R.

**Table 1.** Resolution ( $dx$ ) used for the parameter study and the corresponding time step ( $dt$ ).

$dx$	[ ]	0.05	0.067	<b>0.1</b>	0.13
$dt$	[ ]	0.0125	0.01675	<b>0.025</b>	0.0333

##### 4.2. Reynolds number

The Reynolds number (based on  $R$  and  $U$ ) has earlier been shown to have a small impact on the power coefficient of a single turbine given that it has a minimum value [16]. As the boundary layers are not resolved the flow is in principle inviscid. The Reynolds number can therefore be seen as a numerical parameter rather than a physical parameter. It is needed to stabilize the solution but a too low value will introduce too much diffusion. The Reynolds number is varied in accordance to Table 2, with a reference value of 50000.

**Table 2.** Reynolds number ( $Re$ ) used for the parameter study.

$Re$ [ ]	1000	10000	30000	<b>50000</b>	100000	200000
----------	------	-------	-------	--------------	--------	--------

##### 4.3. Turbulence intensity

The ambient turbulence intensity has an impact on the mixing of the flow and the breakdown of the wake [19][7]. The reference turbulence intensity is set to 6.3 % for the streamwise direction. The value will be varied in accordance to Table 3.

**Table 3.** Measured axial turbulence intensity ( $TI$ ) in the domain, used for the parameter study.

$TI$ [%]	0	3	<b>6.3</b>	11
----------	---	---	------------	----

##### 4.4. Internal spacing

The internal spacing impacts the rate of recovery to the next turbine and the power deficit [23][19]. The reference internal spacing is set to 14 R. The value will be varied in accordance to Table 4. The values correspond to the existing wind farms Lillgrund (LG) and Horns Rev (HR).

**Table 4.** Internal spacing ( $dS$ ) used for the parameter study, with the corresponding cases in the existing wind farms, Lillgrund (LG) and Horns Rev (HR).

$dS$ [ ]	6.6 (LG)	8.6 (LG)	10.6	12.6	<b>14 (HR)</b>	16.6 (HR)	18.8 (HR)	20.8 (HR)
----------	----------	----------	------	------	----------------	-----------	-----------	-----------

## 5. Results

The impact of the different parameters is studied for relative production, wake recovery and turbulence intensity. The relative production is the production of the turbines normalized with the production of the first turbine in the row. The wake recovery shows the wind speed in the streamwise direction ( $z$ ) normalized with the incoming wind speed. The studied turbulence measure is the streamwise "turbulence" (standard deviation of axial wind divided by the mean free stream velocity) and the total "turbulence" (root mean square of the fluctuations for all directions divided by the mean free stream velocity) which both represent the turbulent energy.

### 5.1. Grid resolution

The relative production for turbines 2-5 is lower for higher resolution while for further downstream turbines no clear trend can be seen, see Figure 3. The relative production can also for all resolutions be seen to increase towards the end of the row. The recovery of the streamwise wind speed in the wake behind the wind farm can be seen in Figure 4. The recovery close to the farm seems to be related to the relative production of the last turbines in the farm. Further downstream the wake recovery can be seen to be slower for higher resolutions. The turbulence level is presented in Figure 5. The turbulence level increases through the farm. In the farm wake the levels generally go towards higher values when the grid resolution increases. The turbulence at 6000 m behind the farm ( $z = 276 R$ ) ranges between 5.2 and 6.7 % compared to 6.3 % in the inlet. Overall differences in turbulence are small between the different resolutions.

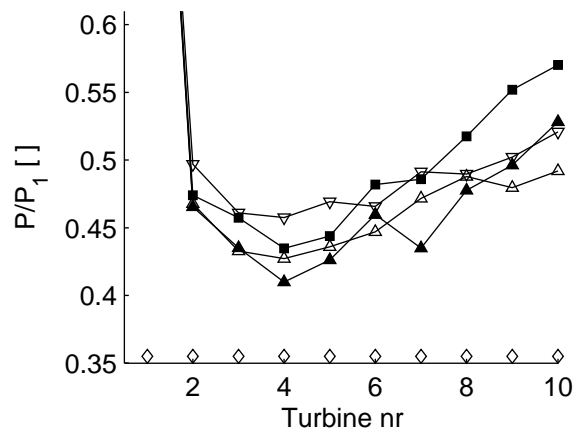


Figure 3. Relative production, turbine 2-10.

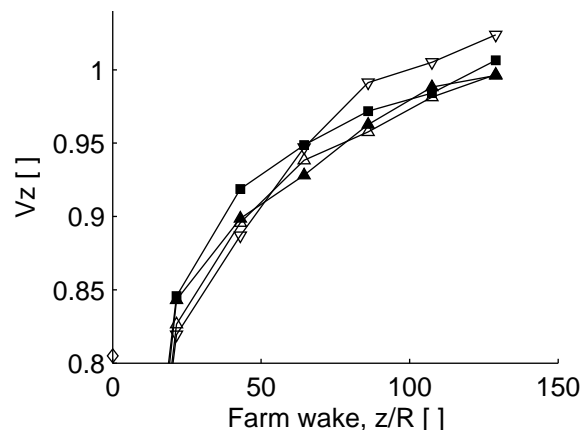


Figure 4. Wake recovery.

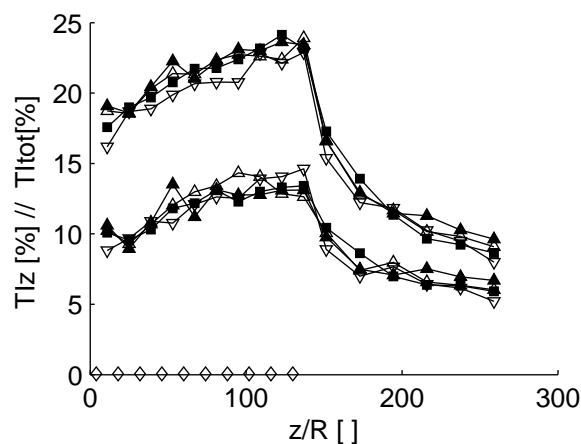


Figure 5. Turbulence intensity.

Figure 3-5. The impact of grid resolution.

#### Legend:

- ▲—  $dx = 0.05 R$
- △—  $dx = 0.067 R$
- $dx = 0.1 R$
- ▽—  $dx = 0.13 R$

Turbine position ( $z$ ) ◇

5.2. Reynolds number

The impact of the Reynolds number on the power coefficient can be seen in Figure 6. The  $C_p$  value for the first turbine decreases as the Reynolds number increases from 1000 to 10000, after that the value is relatively stable with a small decrease for higher Reynolds numbers. For the mean  $C_p$  for all turbines in the row a decrease can be seen up to a Reynolds number value of 100000, after which  $C_p$  starts to increase again. Looking at the relative production in Figure 7 one can see that the values for the first turbines are almost the same apart from when a value of Reynolds number of 1000 is used. For the downstream turbines there is more spread but no clear trend is seen. Studying the wake recovery in Figure 8 it can be seen that the results obtained with  $Re = 1000$  differ here as well, showing a lower wake recovery. It can be seen in Figure 9 that the turbulence levels obtained using  $Re = 1000$  and to some extent 10000 are higher both in the farm and behind.

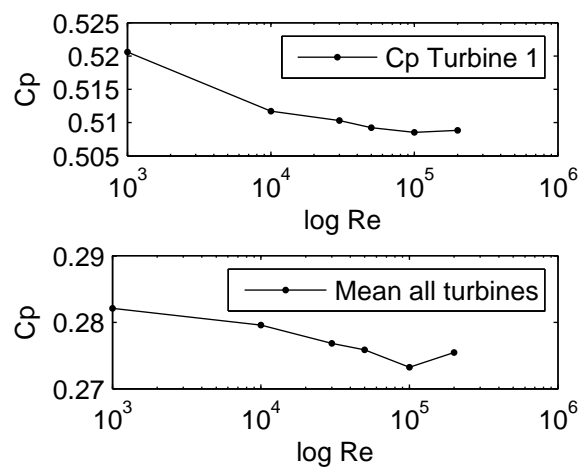


Figure 6. Power coefficient.

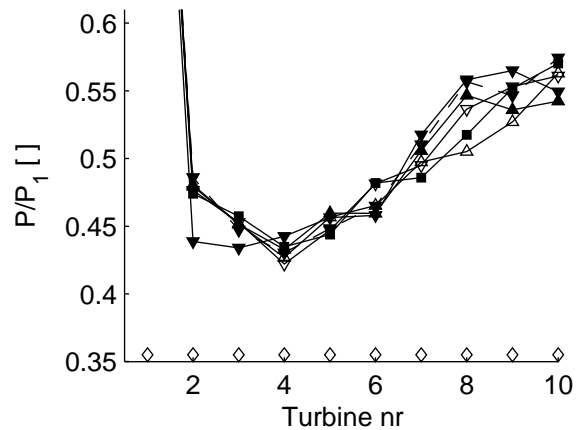


Figure 7. Relative production for turbine 2-10.

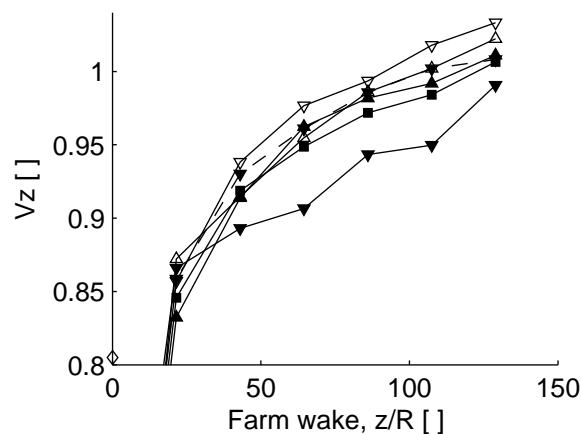


Figure 8. Wake recovery.

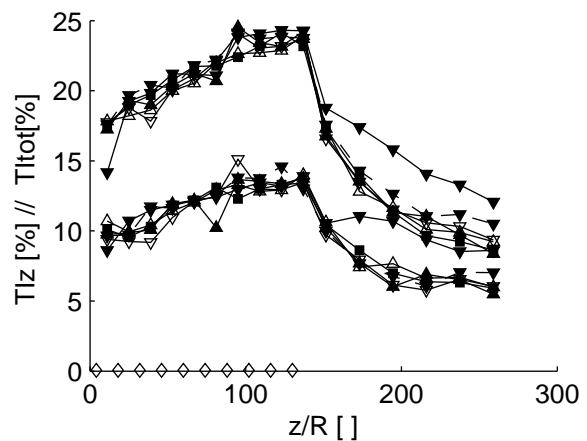


Figure 9. Turbulence intensity.

Figure 6-9. The impact of Reynolds number.

**Legend:**  
 —▲— Re = 200000, —△— Re = 100000, —■— Re = 50000, —▽— Re = 30000, - - - ▼ - - - Re = 10000, —▼— Re = 1000, ◇ Turbine position (z)

### 5.3. Turbulence intensity

The background turbulence level has a high impact on the wake recovery which can be seen in Figure 10. The 0 % and 3 % levels have about the same relative production apart from the second turbine and only a small increase in relative production is obtained for downstream turbines. For higher levels of imposed turbulence the increase in the downstream part of the row is more significant. The wake recovery which can be seen in Figure 11 is significantly impacted by the turbulence level. As expected the higher turbulence levels give faster recovery. It can be seen in Figure 12 that the background turbulence impacts the turbulence level far into the farm. The spread of the turbulence in the farm wake is relatively low and ends up at around 6 % at 6000 m behind the wind farm ( $z = 276 R$ ).

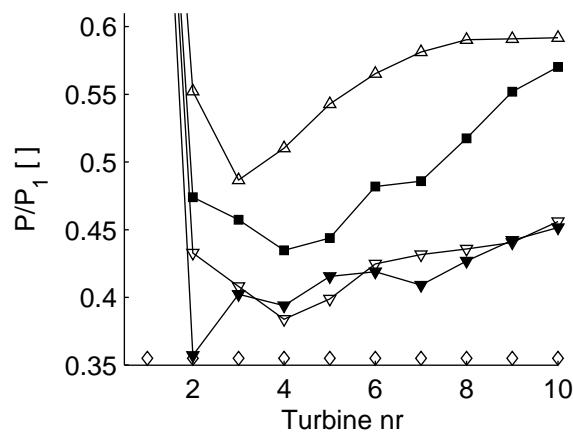


Figure 10. Relative production, turbine 2-10.

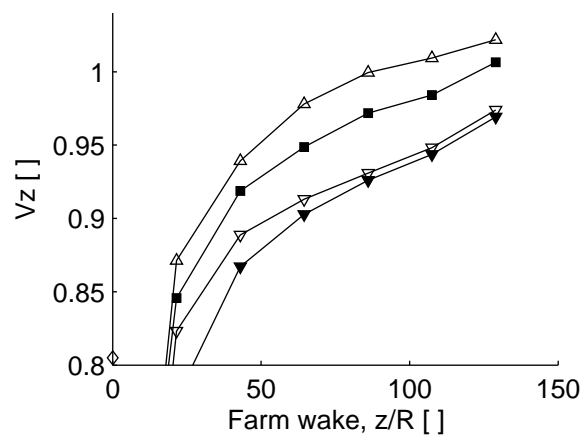


Figure 11. Wake recovery.

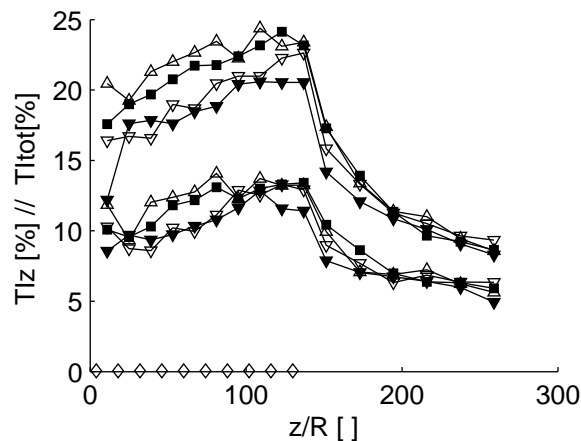


Figure 12. Turbulence intensity.

Figure 10-11. The impact of turbulence intensity.

**Legend:**

- △— TI = 11 %
- TI = 6.3 %
- ▽— TI = 3 %
- ▼— TI = 0 %
- ◇ Turbine position (z)

### 5.4. Internal spacing

The impact of the internal spacing on the wake recovery can be seen in Figure 13. It is interesting to notice that for all cases the axial wind speed behind the farm reaches about the same value after 6 km. It can also be seen that the pace of the wake recovery is higher close behind the farm for shorter spacings. A closer look at the farm wake recovery can be seen in Figure 15. For shorter internal spacings the wind speed in the farm wake does have lower values but the spread is not that large. As can be seen in Figure 14 a higher spacing gives, as expected, a higher relative production. The greatest increase towards the end of the row can be seen for

the intermediate length of internal spacings. The turbulence levels can be seen in Figure 16. Behind the first turbine the levels are clearly dependent on the spacing with higher streamwise turbulence at shorter spacings. For downstream turbines the results show no clear trend.

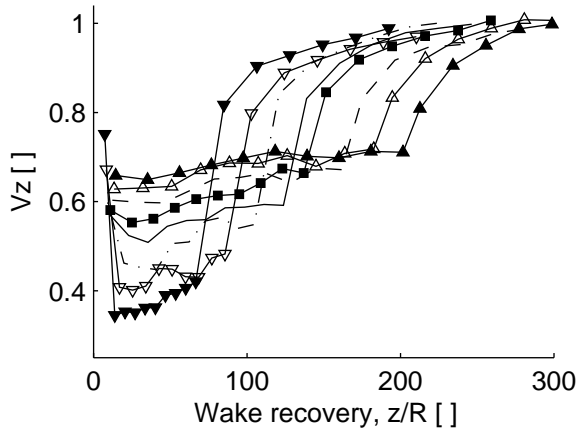


Figure 13. Wake recovery.

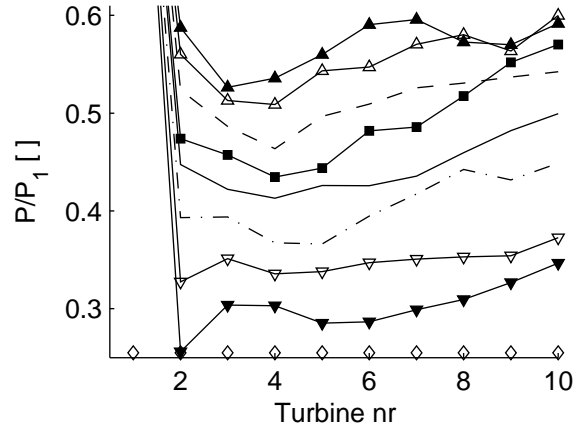


Figure 14. Relative production, turbine 2-10.

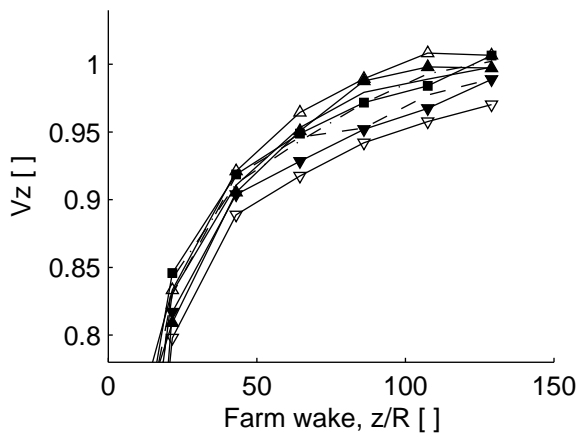


Figure 15. Wake recovery, farm wake.

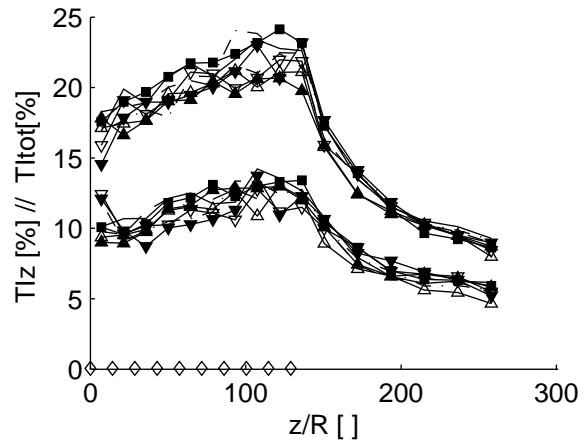


Figure 16. Turbulence intensity.

Figure 13-16. The impact of internal spacing.

Legend:  $\diamond$  Turbine position ( $z$ ),  $\blacktriangle$   $dS = 20.8 R$ ,  $\triangle$   $dS = 18.8 R$ ,  $- - -$   $dS = 16.6 R$ ,  $\blacksquare$   $dS = 14 R$ ,  $\text{---}$   $dS = 12.6 R$ ,  $\cdot \text{---} \cdot$   $dS = 10.6 R$ ,  $\nabla$   $dS = 8.6 R$ ,  $\blacktriangledown$   $dS = 6.6 R$

## 6. Discussion

The background to the paper is the interest in simulations of farm wakes with LES. An earlier study of the wake recovery on Horns Rev showed a higher wake recovery compared to measurements [14]. The aim here was to study the sensitivity and trends in results with different parameter settings for simulations of long distance wakes.

A few trends can be seen in the behavior of the recovery of the farm wake. The resolution does have some impact. A higher resolution gives a slower wake recovery. For the Reynolds number the really small values stand out as expected, but apart from that no clear trend can be seen for the Reynolds number. The level of the background turbulence has a large impact on the relative production and the wake recovery. The turbulence levels inside the farm are also impacted by the background levels, the same impact is not seen for the farm wake. A higher

background turbulence level gives a higher recovery inside and behind the farm. It can also be noticed that a higher background turbulence level gives a clearer trend of increased production downstream in the farm. A larger internal spacing gives a higher wake recovery in the farm wake although the pace is higher close to the farm for shorter spacing. The overall trends are the same for all spacings and the spread is not that large.

In a comparison with experimental data one also needs to consider the impact of atmospheric stability as well as the size and uncertainty of wind direction sectors. The simulations are here done for a fixed wind direction and for neutral conditions. In the work performed in the UpWind project it can be seen that, for the case with 270 degree inflow angle, the relative production is reasonably constant for the downstream rows with neutral/unstable conditions. For a smaller section this is even more the case. A slight increase in production can also be seen in the last rows [24]. The same trend with increasing relative power production in the downstream part of the row can be seen for neutral conditions in meso scale simulations of Horns Rev [25]. Evaluation of the wind direction uncertainty and its impact on wake modeling at the Horns Rev wind farm has been performed [26]. One of the parameters is the variation of incoming wind direction that will cause meandering of the wake [27]. Also earlier work has shown a clear dependency on the inflow angle of the wind [28][24].

A parameter that needs more attention in the simulations is the wind shear. Keck et al. described and verified a method to introduce a prescribed wind shear in combination with pregenerated synthetic turbulence. One of the findings in this work was that the power law shear coefficient used in the prescribed boundary layer definition should be equal to the desired turbulence intensity level in the synthetic turbulence in order to sustain it throughout the computational domain [10]. Troldborg et al. performed further verifications of the prescribed wind shear and the pregenerated synthetic turbulence described in Keck et al. [10] using a simple linear shear approach [11].

## 7. Conclusion

A parameter study of the impact on the wake recovery behind a row of turbines has been performed. Studied parameters were grid resolution, Reynolds number, background turbulence and internal spacing. The most clear impact on the recovery behind the farm could be seen for the background turbulence. A smaller spread in the results could be seen for the other parameters. A lower turbulence level gives slower wake recovery as expected. The background turbulence is also related to the shear in the domain and needs further studies. A slower recovery can also be seen for a higher grid resolution. The slower wake recovery seems to be closer to experimental data from Horns Rev (although the cases are not directly comparable). Changing the Reynolds number, apart from when using the lowest value, leads to small variations in the results. The impact of internal spacing on the wake recovery is small, a shorter spacing gives a slightly slower recovery.

The results of the farm wake recovery show that the used numerical model has a limited dependency on numerical parameters, such as grid resolution, compared to physical parameters, such as internal spacing and turbulence level. Here the Reynolds number could also be considered to be a numerical parameter. For the first turbines in the row the relative production converges when going towards higher grid resolution. The grid dependency further downstream in the farm needs however to be investigated more in detail. Future work will concentrate on investigating if this numerical model can model the boundary layer and farm wake in a physical manner. This study does however indicate that the numerical sensitivity is acceptable.

## Acknowledgments

The simulations were performed on resources provided by the Swedish National Infrastructure for Computing (SNIC) at the National Supercomputer Centre in Sweden (NSC)

## References

- [1] Frandsen S, Barthelmie R, Rathmann O, Jørgensen H, Badger J, Hansen K, Ott S, Rethore P, Larsen S and Jensen L 2007 *Summary report: The shadow effect of large wind farms: measurements, data analysis and modelling*. (Risø-R-1615(EN), Denmark)
- [2] Crespo A, Hernández J and S F 1999 *Survey of modelling methods for wind turbine wakes and wind farms*. (Wind Energy 1999 ; 2: 1–24)
- [3] Vermeer L, Sørensen J and Crespo A 2003 *Wind turbine wake aerodynamics*. (Progress in Aerospace Sciences 2003; 39: 467–510.)
- [4] Barthelmie R, Hansen K, Frandsen S, Rathmann O, Schepers J, Schlez W, Rados K, Zervos A, Politis E and Chaviaropoulos P 2009 *Modeling and measuring flow and wind turbine wakes in large wind farms offshore*. (Wind Energy 2009; 12: 431–444.)
- [5] Ivanell S 2009 *Numerical Computations of Wind Turbine Wakes*. (PhD thesis, ISBN 978-91-7415-216, KTH Engineering Sciences, Sweden)
- [6] Lu H and Porté-Agel F 2011 *Large eddy simulation of a very large wind farm in a stable atmospheric boundary layer*. (Physics of Fluids 2011; 23: 065101)
- [7] Wu Y T and Porté-Agel F 2012 *Atmospheric turbulence effects on wind-turbine wakes: An LES study*. (Energies 2012, 5, 5340-5362)
- [8] Troldborg N, Sørensen J and Mikkelsen R 2010 *Numerical simulations of wake characteristics of a wind turbine in uniform inflow*. (Wind Energy 2010; 13: 86–99)
- [9] Troldborg N, Larsen G, Hansen K, Sørensen J and Mikkelsen R 2011 *Numerical simulations of wake interaction between two wind turbines at various inflow conditions*. (Wind Energy 2011; 14: 859–876.)
- [10] Keck R E, Mikkelsen R, Troldborg N, de Maré M and Hansen K 2013 *Synthetic atmospheric turbulence and wind shear in large eddy simulations of wind turbine wakes*. (Wind Energy 2013; DOI: 10.1002/we.1631)
- [11] Troldborg N, Sørensen J N, Mikkelsen R and Sørensen N N 2013 *A simple atmospheric boundary layer model applied to large eddy simulations of wind turbine wakes*. (Wind Energy)
- [12] Nilsson K, Ivanell S, Hansen K, Mikkelsen R, Breton S P and Henningson D 2014 *Large-eddy simulations of the Lillgrund wind farm*. (Wind Energy 2014; DOI: 10.1002/we.1707)
- [13] Brand A 2009 *Wind Power Plant North Sea – Wind farm interaction, The effect of wind farming on mesoscale flow*. (ECN, the Netherlands)
- [14] Eriksson O, Mikkelsen R, Nilsson K and Ivanell S 2012 *Analysis of long distance wakes of Horns rev 1 using actuator disc approach*. (The Science of Making Torque From Wind, 2012)
- [15] Breton S P, Nilsson K, Olivares-Espinosa H, Masson C, Dufresne C and Ivanell S 2013 *Study of the influence of atmospheric turbulence on the asymptotic wake deficit in a very long line of turbines*. (ICOWES 2013)
- [16] Mikkelsen R 2003 *Actuator Disc Methods Applied to Wind Turbines*. (DTU, Denmark)
- [17] Mann J 1998 *Wind field simulation*. (Risø, Denmark)
- [18] TaPhouc L 1994 *Modèles de sous maille appliqués aux écoulements instationnaires décollés*. (Tech. rep. LIMSIS 93074 LIMSIS France.)
- [19] Hansen K S, Barthelmie R J, Jensen L E and Sommer A 2012 *The impact of turbulence intensity and atmospheric stability on power deficits due to wind turbine wakes at Horns Rev wind farm*. (Wind Energ., 15: 183–196.)
- [20] Jonkman J, Butterfield S, Musial W and Scott G 2009 *Wind Turbine for Offshore System Development*. (NREL, the United states of America)
- [21] Breton S P, Nilsson K, Ivanell S, Olivares-Espinosa H, Masson C and Dufresne L 2012 *Study of the effect of the presence of downstream turbines on upstream ones and use of a controller in CFD wind turbine simulation models*. (Proceeding of The Science of Making Torque from Wind, 2012.)
- [22] Jakob M, Ott S, Jørgensen B H and Frank H P 2013 *WAsP Engineering 2000*. (Risø–R–1356(EN))
- [23] Barthelmie R J and Jensen L E 2010 *Evaluation of wind farm efficiency and wind turbine wakes at the Nysted offshore wind farm*. (Wind Energ., 13: 573–586.)
- [24] Hansen K S, Barthelmie R, Cabezon D and Politis E 2008 *Wp8: Flow Deliverable D8.1 Data Wake measurements used in the model evaluation*. (DTU.)
- [25] Baltscheffsky M, Söderberg S, Bergström H and Svensson N 2013 *Using a mesoscale atmospheric model to study wind turbine wakes and farm-farm interaction*. (EAWC Offshore 2013)
- [26] Gaumont M, Réthoré P E, Ott S, Peña A, Bechmann A and Hansen K S 2013 *Evaluation of the wind direction uncertainty and its impact on wake modeling at the Horns Rev offshore wind farm*. (Wind Energ.. doi: 10.1002/we.1625)
- [27] Larsen G C and et al 1994 *Dynamic wake meandering modeling*. (Risø-R-1607(EN) Denmark.)
- [28] Ivanell S, Mikkelsen R, Sorensen J N, Hansen K S and Henningson D 2009 *The impact of wind direction in atmospheric BL on interacting wakes at Horns Rev wind farm*. (PhD thesis, ISBN 978-91-7415-216, KTH Engineering Sciences, Sweden)